SSC-187

The Superconducting Super Collider

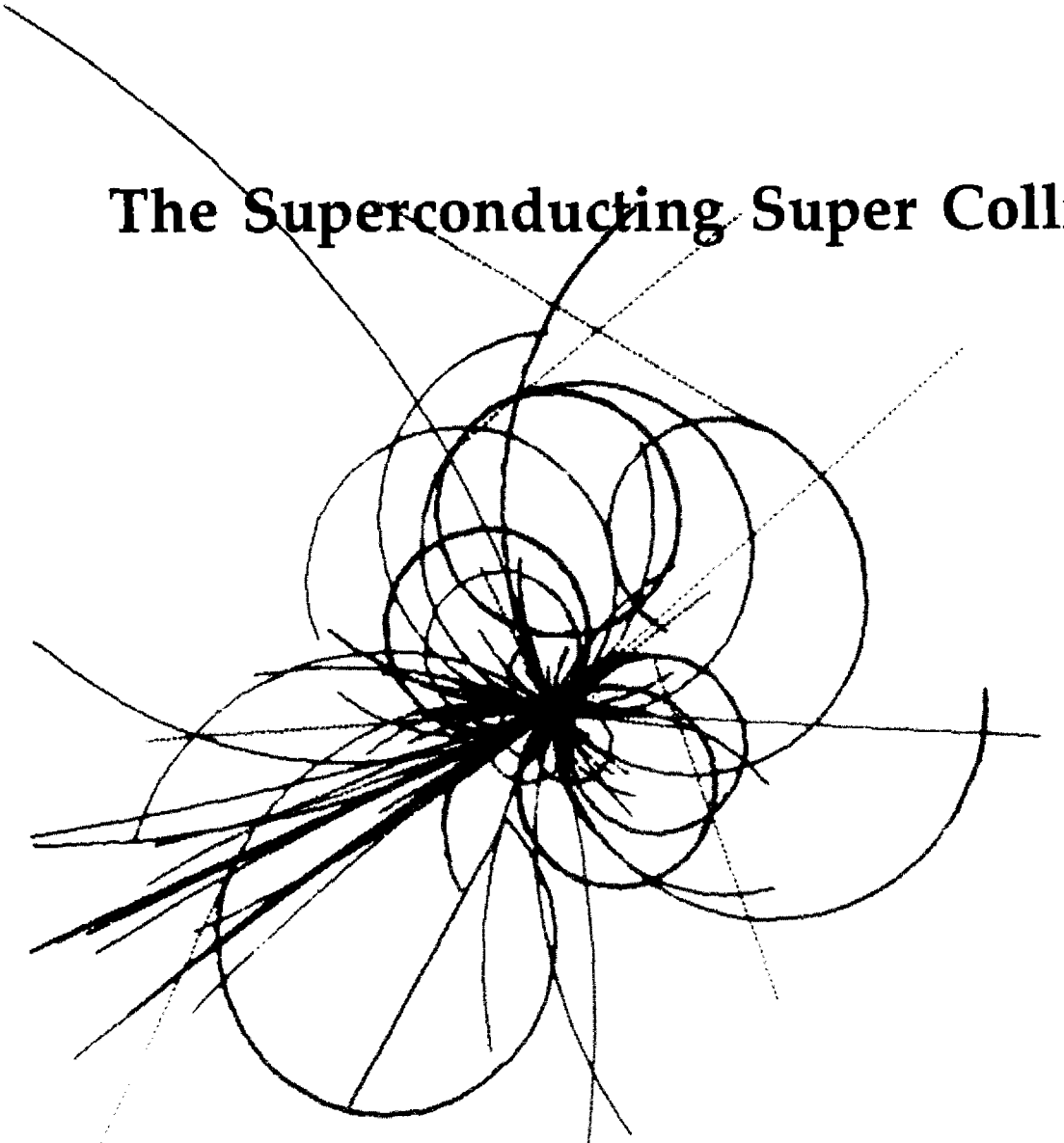

Brief Comments on Nonlinear Dynamics Studies in Storage Rings

A.W. Chao
SSC Central Design Group

September 1988

SSC-187

BRIEF COMMENTS ON NONLINEAR DYNAMICS STUDIES IN STORAGE RINGS*

A. W. Chao
SSC Central Design Group†

September 1988

*Submitted to the 1988 Applied Superconductivity Conference, San Francisco, CA, September 21–26, 1988

†Operated by Universities Research Association for the U. S. Department of Energy

BRIEF COMMENTS ON NONLINEAR DYNAMICS STUDIES IN STORAGE RINGS

A. W. Chao
SSC Central Design Group
c/o Lawrence Berkeley Laboratory
One Cyclotron Road
Berkeley, California 94720

Abstract

A few comments on the subject of single particle nonlinear dynamics in storage rings are presented.

Introduction

If the accelerator optics is perfectly linear, the trajectory of a particle traces out a circle in the normalized phase space (q,p), as shown in Fig. 1(a). The tune v (phase advance per turn /2π) is independent of the initial coordinates of the particle. We assume v is an irrational number.

The picture becomes complicated when a nonlinear perturbation is added to the system. The first complication is the introduction of tune shift. For particles near the phase space origin, the tune remains v, but as the particle amplitude A increases, the tune shifts. As the tune changes, it can no longer stay irrational. The phase space trajectories then look like Fig. 1(b). Circles are trajectories of particles that have irrational tunes. Discrete dots belong to those with rational tunes. As the tune varies between irrational and rational values, the phase space looks like an infinitely layered sandwitch.

But the nonlinear perturbation has another much nastier effect. Around each discrete dot corresponding to a rational tune, an island of finite area is created, and immediately outside the islands is a thin chaotic layer in which the turn-by-turn trajectory does not follow a smooth pattern. The existence of chaotic layers is the signature that the system is not integrable. As the islands acquire finite sizes, they break the neighboring circles.

The islands and chaotic layers emerge spontaneously in the entire phase space, even close to the origin. However, by its nature, the nonlinearity has only a weak effect at small amplitudes. This means islands near the origin are extremely thin, and most invariant surfaces are able to maintain their existence (the KAM surfaces[1]) and suffers only from a small distortion from a circle. The distorted circles constitute invariant surfaces. The significance of invariant surface is that once it exits, all particles inside of it will not leak out, thus assuring their stability.

The percentage distortion from circles is called the "smear." As the amplitude increases, the islands grow in size, breaking more invariant surfaces.[2] However, not all circles are created equal. Some of them correspond to tunes that are more irrational than others, and they tend to break later than others. These tunes are those containing a $\sqrt{5}$ in the form $(n+m\sqrt{5})/k$, where n, m, and k are integers. So, as the islands grow in size, these invariant surfaces persist for a while, but they are now more distorted from circles, i.e., the smear has increased. Figure 1(c) is a sketch of islands and chaotic layers.

As amplitude increases further, even the persistent invariant surfaces are broken by neighboring island chains which are now large enough to "overlap." Beyond that point, the phase space looks like Fig. 1(d). The islands still exist, but they now become disjoint, and they are embedded in a chaotic ocean. Particle motion is no longer bounded and instabilty occurs. The last invariant surface is called the "dynamic aperture."

Instead of Fig. 1(d), a situation illustrated in Fig. 2(a) could happen. An invariant surface exists, but before the islands overlap, the tune shift with amplitude runs out of steam to close the islands from above and the dynamic aperture is reached prematurely. In practice, this is the situation to be avoided by properly choosing the nominal tune (except for resonance beam extraction in synchrotrons). To avoid the situation shown in Fig. 2(a) is to avoid resonances by choosing the tune so that 2(a) looks more like 2(b).

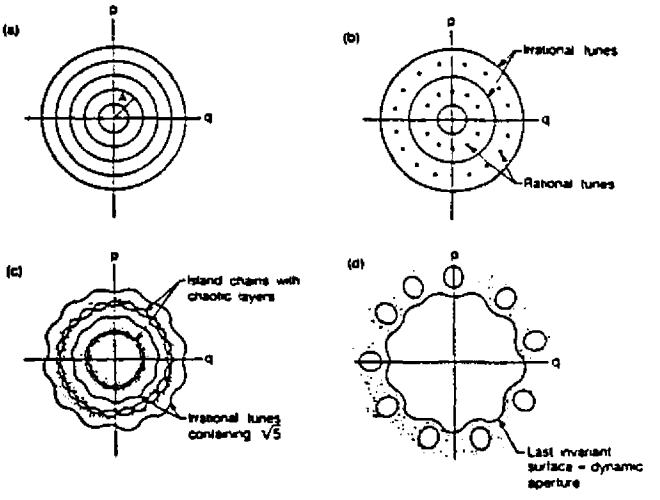

Fig. 1. (a) Phase space trajectories in a linear system when the tune is an irrational number. (b) Tune shift makes the phase space an infinitely layered structure of circles and discrete dots. (c) Islands and chaotic layers surround the discrete dots, breaking some of the circles and distorting others. (d) When the amplitude is large enough, all circles are broken, resulting in a dynamic aperture.

We have thus identified several effects in an accelerator with nonlinear perturbations: Δv(A), smear (A), islands and chaotic layers, and the dynamic aperture. Nonlinear dynamics is clearly quite complicated. It becomes even more so if more than 1-D is being considered. The most pronounced difference is that the existence of KAM surface means bounded motion for 1-D case (or 2-D case with a time-independent Hamiltonian). Beyond 2-D, however, the invariant surfaces do not forbid particles leaking through intricate channels connecting the inside phase space to the outside (Arnold diffusion[1]).

Canonical Perturbation Theory[3,4,5,6]

Conventionally, theoretical studies of nonlinear dynamics are made using perturbation theories. The idea is to first insist that the system remains integrable under the nolinear perturbation, and look for the invariant surfaces perturbatively. When a convergent solution is found, an invariant surface exists. Otherwise, an invariant surface does not exist and

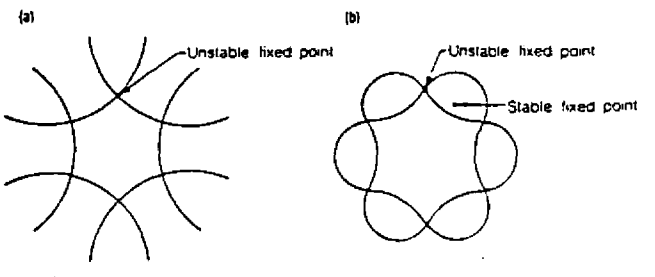

Fig. 2. Phase space topology can be either (a) open or (b) closed. Case (a) is in general to be avoided by avoiding the low order resonances.

one is in a chaotic region. Roughly speaking, there are two situations when the system is integrable: either when one is "away from all resonances," or there is only one "single, isolated resonance" nearby. It is therefore in these regimes where a perturbative theory usually applies. One moment's reflection shows these can at best be qualitative description since there is always an infinite number of resonances infinitely close by.

The classical treatment is the canonical perturbation theory. It starts with a Hamiltonian

$$H = H_0(J) + \varepsilon V(\phi, J, \theta) \tag{1}$$

where J and ϕ are the action-angle variables, V is the nonlinear perturbation which is periodic in the time variable θ. The unperturbed Hamiltonian H_0 includes the tune shift effect with $\nu(J)=dH_0/dJ$. A review of alternative perturbation approaches can be found in Ref. 5.

The trick is to try to make a canonical transformation from (J, ϕ) to (J_1, ϕ_1) by a generating function. The transformation is chosen in such a way that the θ and ϕ dependencies are removed so that we end up with a Hamiltonian which is a function of J_1 alone. This can be done perturbatively. To first order in ε, this is done by choosing the generating function

$$F(\phi, J_1, \theta) = \phi J_1, + \varepsilon G(\phi, J_1, \theta) \tag{2}$$

with

$$G(\phi, J_1, \theta) = \sum_m \frac{i}{2 \sin \pi m \nu} \int_\theta^{\theta+2\pi} d\theta' \, v_m(J_1, \theta') \, e^{im[\phi+\nu(\theta-\theta'-\pi)]} \tag{3}$$

where $v_m(J, \theta)$ is the m^{-th} Fourier component of V. The transformed Hamiltonian is

$$H_1(J_1, \phi_1, \theta) = H_0(J_1) + O(\varepsilon^2) \tag{4}$$

The perturbation is now second order in ε. If this is ignored, we have J_1= constant of the motion, and the problem is solved. In particular, the phase space contours are just the J_1 contours. Note that since $J = J_1 + \varepsilon \, \partial G/\partial\phi_1$, the term $\varepsilon \, \partial G/\partial\phi_1$ gives the first order expression of the smear.

There are two approaches to proceed to higher orders. One is to expand G in power series of ε and deal with the canonical transformation order by order. After n steps, the Hamiltonian has a perturbation of order ε^{n+1}. The other approach, called "superconvergent,"[7] is to iterate first order perturbations but to start fresh after each iteration. After n iterations, the perturbation is of the order ε^{2**n}. Again, once the invariant surface is obtained, the problem is in principle solved.

Resonances

The problem with the perturbation method is that the process may not converge. The problem is that of small denominators. An indication has occurred in the expression of the generating function, Eq. (3), which diverges when

$$m \nu = \text{integer}, \tag{5}$$

or equivalently, when ν = rational number. Canonical perturbation theory therefore breaks down near resonances. An implicit assumption when writing down Eq. (3) is therefore that one is "away from all resonances". The fact that there are resonances arbitrarily close by is presumably compensated by the fact that these arbitrarily high order resonances are also infinitely weak. In practice, they are therefore simply ignored.

One does well also in the other extreme, i.e., when the dynamics are dominated by a single isolated resonance, say $\mathbf{m}.\nu$ = integer. In that case, we could try at least to remove the θ dependence to first order in ε, yielding

$$H = H_0(J) + \varepsilon V(J) \cos(\mathbf{m}.\phi) + O(\varepsilon^2) \tag{6}$$

The bold quantities ν, m, and J represent vectors in multi-dimensional case. One constant of the motion is H itself. In 1-D case, this assures integrability. Whether the motion is bounded or not depends on the topology of the H contours, as shown in Fig. 2.

In the 2-D case, near the resonance $m_x\nu_x+m_y\nu_y$ = integer, the Hamilton's equation $J'=-\partial H/\partial\phi$ gives $J_x'/m_x=J_y'/m_y$ which in turn yields an additional invariant condition

$$m_y J_x - m_x J_y = \text{invariant}. \tag{7}$$

Since $J_{x,y} > 0$, this leads to the well known[8] conclusion that sum resonances are unbounded while difference resonances are bounded.

If one of the two dimensions is the synchrotron dimension, near the resonance $m_x\nu_x+m_s\nu_s$ = integer, the invariant condition becomes

$$m_s J_x \pm m_x J_s = \text{invariant} \tag{8}$$

where $\pm$ means above and below transition, respectively. The change of sign above transition is a consequence of the negative longitudinal mass. Above transition, motion is therefore bounded near sum resonances and unbounded near difference resonances.[9]

In the 3-D case near a resonance $m_x\nu_x+m_y\nu_y+m_s\nu_s$ = integer, Hamilton's equation gives $J_x'/m_x=J_y'/m_y=\pm J_s'/m_s$. It follows that unbounded motion occurs when

- all m_x, m_y and m_s are of the same sign if below transition
- m_x and m_y are of the same sign, m_s has opposite sign if above transition. (9)

All other sign combinations give bounded motion. It should be pointed out, however, that bounded motion does not necessarily mean stability in practice. This is because the a small decrease in one dimension may allow the other dimension to grow by a large amount, thus exceeding the aperture. This is especially the case when longitudinal dimension is involved.

Hamilton-Jacobi Equation[10]

It was pointed out that the canonical perturbation theory is just a perturbative way to solve the Hamilton-Jacobi equation, so why not try to solve it directly numerically rather than perturbatively. This leads to the Hamilton-Jacobi equation for $G(\phi, J_1, \theta)$,

$$H_0(J_1+\partial G/\partial\phi) + V(\phi, J_1+\partial G/\partial\phi, \theta) + \partial G/\partial\theta$$

$$= \text{function of } J_1 \text{ alone, i.e., new Hamiltonian } H_1(J_1) \tag{10}$$

The job is to solve for G using the above nonlinear partial differential equation. The condition is that the m-th Fourier component of the left hand side of Eq. (10) vanish for all nonzero m. In practice, the Fourier expansion is of course terminated by a truncation. Note that the task is not as formidable as it might seem due to the fact that J_1 is an invariant and acts as an input parameter. The direct solution of the H-J equation seems to offer a promising approach to realistic nonlinear accelerator problems.

Figure 3 is the result of applying this technique to a simple example of an integrable Hamiltonian that describe a single isolated 4-th order resonance. Separatrices can not be calculated due to small denominators. But by approching the separatrix, one obtains Fig. 3(a), which can be compared with the Hamiltonian contours, Fig. 3(b), obtained from the exact analytical expression.

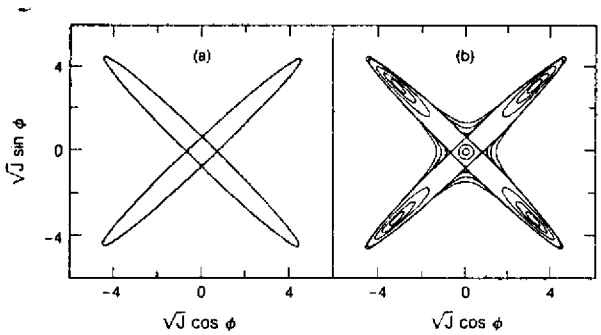

Fig. 3. (a) Contour obtained by directly solving of the Hamilton-Jacobi equation. (b) Contours using exact analytic expression.

Tracking Simulations

An indispensable tool for studying nonlinear dynamics in accelerators is to simulate particle motion by tracking. Typically, one first models the accelerator lattice, chooses the initial conditions of the particles, and then tracks the trajectory of these particles by a computer code.

The difficult job of preparing a tracking code is not so much of developing the code itself. Rather it is to decide on the tradeoff between computing speed and the degree of simplification of the lattice model. The decision of course depends on the envisioned purpose of the tracking code. For storage ring applications, practically all tracking codes assume drastically simplified models of one type or another: ignoring fringe fields, kick approximation for nonlinear elements, simplified Hamiltonian, concatenated maps to represent the dynamics for one revolution, etc. Other than some detailed features, these simplifications are mostly acceptable, and in any case necessary for applications to large storage rings and/or to study long term effects.

The full expression of the Hamiltonian is[11]

$$H = \frac{x}{\rho} + \frac{x^2}{2\rho^2} - \left(1 + \frac{x}{\rho}\right)\sqrt{(1+\delta)^2 - x'^2 - y'^2} + \frac{eA_s}{P_o c} - \frac{z'}{\beta_o} \qquad (11)$$

with canonical variables (x, x', y, y', z, z') and δ related to z' by $(1+\delta)^2 = 1 - 2z'/\beta_o + z'^2$.

Even in the absence of nonlinear elements (e.g., sextupoles), Eq. (11) shows that there are nonlinear terms due to kinematics. However, for large storage rings, they are often ignored by expanding the square root in power series and keep up to second order in x' and y'. All nonlinearities then come from A_s. This gives a simplified Hamiltonian

$$H \approx \frac{x'^2 + y'^2}{2(1+\delta)} - \delta + 1 - \frac{z'}{\beta_o} \qquad \text{drift}$$

$$- \delta x/\rho + x^2/2\rho^2 \qquad \text{sector bends}$$

$$+ eA_s/P_o c \qquad \text{other elements} \qquad (12)$$

In particular, thick bends is treated as a linear element using Eq. (12).

Equation (12) is adopted by most tracking codes. An alternative approach, adopted for example by TEAPOT,[12] is to model all beam line elements (including bends) as thin lenses. This allows keeping the exact Hamiltonian [Eq. (11)] because it is needed only in drift spaces.

Explicit Canonical Integration[11,13]

Thin lens approximation to a given element, linear or nonlinear, is the lowest order (in element length) approximation. To improve the accuracy for a thick lens magnet of length L and integrated strength LS, one way is to split the element into a number of evenly spaced slices. But faster convergence can be obtained with canonical integration techniques. For example,

model	error
(L) (SL)	$O(L^2)$
$\left(\frac{L}{n}\right)\left(\frac{SL}{n}\right)$ ... repeated n times	$O(L^2/n)$
$\left(\frac{L}{2}\right)$ (SL) $\left(\frac{L}{2}\right)$	$O(L^3)$
$\left(\frac{L}{2n}\right)\left(\frac{SL}{n}\right)\left(\frac{L}{2n}\right)$ ... repeated n times	$O\left(\frac{L^3}{n^2}\right)$
$(L_1)(S_1L)(L_2)(S_2L)(L_2)(S_1L)(L_1)$	$O(L^5)$

where (L) means a drift of length L, (SL) means a thin lens element whose integrated strength is SL, $L_1 = L/2(2-b)$, $L_2 = L(1-b)/2(2-b)$, $S_1 = S/(2-b)$, $S_2 = Sb/(2-b)$, $b = 2^{1/3}$. Note that the more pieces the element is broken into, the higher the precision is. Also note that symmetry always gives one order higher than otherwise. Armed with the canonical integration technique (of which thin lens approximation is one example), a thick nonlinear element (with the exceptions of fringe fields and undulators) can be modeled.

Taylor and Lie Maps[14,15,16]

The beam dynamics between two positions in an accelerator can be represented by the map between these two positions (Twiss analysis is an example in the linear case). One special case of such maps is that representing one complete turn of the accelerator. Several beam dynamics quantities can be extracted from this one-turn map: tune shifts with betatron amplitudes and momentum, smear as a function of amplitudes, distortion functions, strengths of nonlinear resonances, etc. Thus the one-turn map is ideal for various analytical studies of the nonlinear dynamics of the accelerator. In addition, it also offers the possibility to perform fast particle tracking because the entire accelerator is now modelled as a single map. This later possibility, however, has to be taken with care.

There are two common approaches to obtain a one-turn map. One is to use the generating function obtained in the canonical perturbation theory or the direct solution of the Hamilton-Jacobi equation, as discussed before (but with slightly different boundary conditions). The other way, which is discussed next, is to represent the map by power series. For example, the final coordinate of a particle can be written as a Taylor series in terms of the initial coordinates. This will be referred to as a Taylor map. Another example is to represent the map as a Lie operator exp(:F:), where F is written as a power series. Example programs using Taylor maps are TRANSPORT[17] and COSY[18]. An example using Lie maps is MARYLIE.[19]

The Taylor and Lie maps are in principle equivalent ,and they can be transformed into each other whenever desirable. However, there are practical differences. The advantage of a Taylor map is that it is easy to obtain in a code—just keep substituting the exit coordinates into the entrance coordinates of the next beam line element and truncate the final expression to the order of interest. (This is especially true when Eq. (12) is used as the Hamiltonian and the elements are represented as kicks using canonical integration techniques). Also, it is easy to apply in particle tracking.

The transformation of a thick element with Hamiltonian H is simply exp(-:HL:) in the Lie representation. But concatenation of two elements is not as straightforward as the Taylor method. An advantage of Lie representation is that it is more concise. The number of coefficients needed to represent an n-th order map in a m-dimensional phase space is less than the corresponding number in a Taylor map:

Taylor maps:

	n=1	n=2	n=3	n=4	n=5
m=2	4	10	18	28	40
4	16	56	136	276	500
6	36	162	498	1254	2766

Lie maps:

	n=1	n=2	n=3	n=4	n=5
m=2	3	7	12	18	25
4	10	30	65	121	205
6	21	77	203	455	917

Formally, Lie representation is automatically symplectic. However, in actual tracking applications, artificial symplectification has to be applied even in a Lie environment. Another important advantage of the Lie representation is that the one-turn map is obtained in the Lie format is ideal for analysis purposes.

Judging from the above comparison between the Taylor and the Lie representations, it seems that a practical, efficient method would be a hybrid combination of these techniques:

- adopt the canonical integration for beam line elements,
- use kick code to generate the Taylor map for one turn,
- transform the Taylor map into a Lie map,
- analyze with the Lie map, (13)
- when judged appicable, track with the symplectified Taylor map.

The larger storage space needed for the Taylor map coefficients is not regarded as serious in this approach. This hybrid approach is being adopted for the SSC studies.

Differential Algebra[15,16]

The above scheme is greatly enhanced by the existence of an efficient technique, based on differential algebra, that generates the one-turn Taylor map. To describe this technique, first consider a tracking (or ray tracing) program hat starts with initial condition (x_0, x'_0) and follows the particle through beam line elements (or integration steps) as follows

$$(x_0, x'_0) \rightarrow (x_1, x'_1) \rightarrow (x_2, x'_2) \ldots \rightarrow (x_N, x'_N) \quad (14)$$

element 1 element 2 element N

The same steps are followed in the differential algebra approach. The only difference is that the initial X_0 is now taken to be a set of numbers arranged in a vector form (1, 0, 0, ..., 0) and X'_0 is now (0, 1, 0, ..., 0). (A capitalized letter means vector here.) The number of entries in the vector depends on the desired order of the map. To go through element 1, these vectors are substituted into the same expressions as the tracking program. Rules are defined for the various operations (addition, multiplication, square root, sine, cosine, etc.) on the vector numbers. After going throught element 1, one obtains X_1 and X_1, whose entries are now no longer 0's and 1's. The vectors X_1 and X_1 are then substituted into expressions for element 2, and the procedure continues until the end of beam line, or end of ray tracing steps.

Miraculously, after this process, the numbers in the final X_N and X'_N vectors have the significance as shown below:

$$X_N = (\partial x_N/\partial x_0, \partial x_N/\partial x'_0, \partial^2 x_N/\partial x_0^2, \partial^2 x_N/\partial x_0 \partial x'_0, \partial^2 x_N/\partial x_0'^2, \ldots)$$

$$X'_N = (\partial x'_N/\partial x_0, \partial x'_N/\partial x'_0, \partial^2 x'_N/\partial x_0^2, \partial^2 x'_N/\partial x_0 \partial x'_0, \partial^2 x'_N/\partial x_0'^2, \ldots) \quad (15)$$

where the derivatives are evaluated at the origin (or the closed orbit). The algebra does not require numerical differentiation involving subtracting numbers that are almost equal and thus all derivatives are accurate to computer accuracy. Once the derivatives are obtained, the Taylor map follows. By keeping more entries in the vector, maps of arbitrarily high orders can be obtained. This is by far the most efficient way of generating maps. An exaggerated example, the map for a 90° bend up to 50th order, is given below:[20]

order	$(x\|x'^n)$	order	$(x\|x'^n)$
0	0.000000E+00	1	0.500000
4	–.625000E–01	6	–.312500E–01
8	–.954861E–02	10	–.438368E–02
12	–.175964E–02	14	–.494470E-03
16	–.120357E–03	18	–.303507E-04
20	–.748015E–05	22	–.166065E-05
24	–.340812E–06	26	–.682165E–07
28	–.133936E–07	30	–.252307E–08
32	–.454204E–09	34	–.792470E–10
36	–.135272E–10	38	–.225391E–11
40	–.365251E–12	42	–.576846E–13
44	–.891832E–14	46	–.135248E–14
48	–.201106E–15	50	–.293181E–16

Note that the differential algebra tool has been developed for 6-D phase space. (Dimensions >6 have been implemented to include dependence of the map on external parameters such as the strength of a particular nonlinear element.) Equation (15) is the special case for 2-D. Note also this tool itself does not constitute a program; it is to be attached to an existing tracking or ray tracing program, precompiled, and it will then generate the map corresponding to the case being simulated. Finally, the elements do not have to be magnet multipoles. For example, a beam-beam kick could be treated as one of the elements.

E778

Experiments have been carried out in accelerators to study nonlinear dynamics in the past, and more recently at SpS,[21,22] SPEAR,[23] and Tevatron.[24] Here we will briefly mention a recent formal experiment at the Tevatron, the Experiment E778.[25,26,27]

In a typical E778 run, a beam is first injected at 150 GeV. A set of 16 intentional sextupoles are turned on, and at the flat top of the sextupole strength, the beam is kicked horizontally. The subsequent motion of the beam is then monitored by two beam position monitors approximately 90° out of phase. Polarities of the sextupoles are such that ideally no net change of chromaticities occur. The (x_1, x_2) information turn after turn can be transformed into a normalized phase space. When sextupoles are turned off, the trajectory traces out a circle, as shown in Fig. 4(a). When sextupoles are turned on, the circle is distorted (in this case into a triangular shape), as shown in Fig. 4(b). The percentage distortion gives the smear at the amplitude corresponding to the strength of the kick.

Figure 5 is a compilation of the results of several such runs. It shows the smear as a function of sextupole strength for 3 kick amplitudes. The smear increases with sextupole strength, as well as the kick amplitude, as one would expect. The solid lines are obtained by tracking simulation. The agreement with experimental data is quite reasonable.

The phase space actually has a richer structure than Fig. 4 might suggest. For example, when tune is close to 2/5, a chain of five islands is formed in the phase space. Figure 6 shows the detailed phase space obtained by tracking. Both the triangular and the five-island structures are present. When the beam is kicked to an amplitude so as to overlap one of the islands, part of the beam will be locked onto the island and will exhibit the island structure in its subsequent motion. Figure 7 is an observation in E778 which dramatically demonstrates this behavior. This is a dramatic direct observation of the existence of islands in a nonlinear dynamical system.

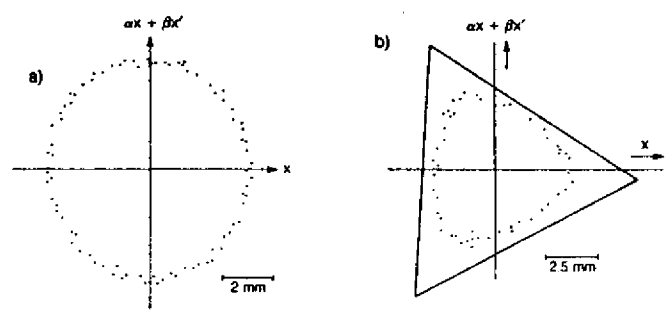

Fig. 4. Experimenal observation of beam trajectory in normalized phase space at the Tevatron. (a) Experimenal sextupoles are turned off. (b) Trajectory is distorted when 8 sextupoles are turned on. The tune is near 1/3. The triangle is the calculated separatrix.

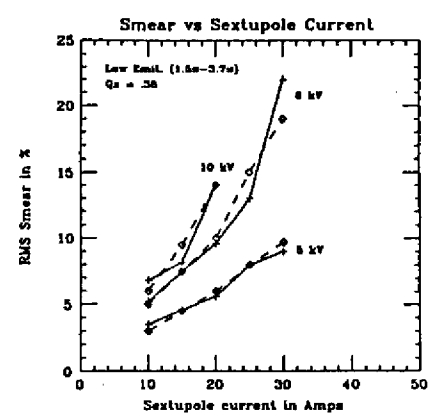

Fig. 5. Smear versus sextupole strength in E778 for three kicker strengths (in kV units). Solid lines are simulation results.

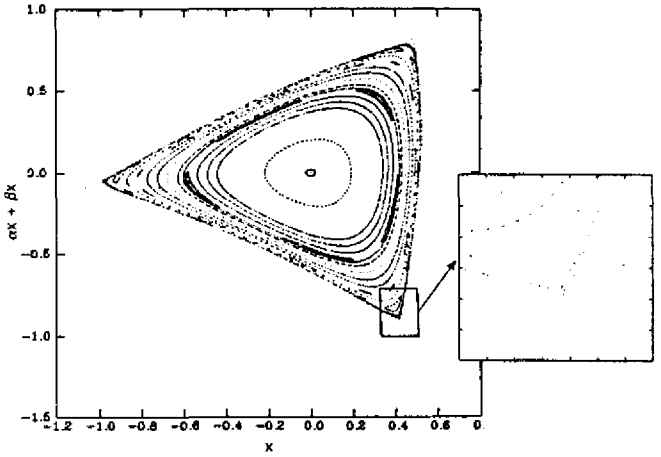

Fig. 6. Detailed phase space structure obtained by tracking when sextupoles are set to 25 amperes.

Fig. 7. When the tune is near 2/5, the kicked beam exhibits a five-island structure in the (x_1, x_2) space.

References

[1] See, for example, V. I. Arnold, "Mathematical Methods of Classical Mechanics", Springer-Verlag, 1978.

[2] See, for example, R. S.MacKay, Lecture Notes in Phys. 247, Springer-Verlag 1985, p. 390.

[3] For a review, see R. D. Ruth, AIP Proc. 153 (1987), 150.

[4] L. Michelotti, Part. Accel. 19, 205 (1986).

[5] G. Guignard, Workshop on Aperture Limitations in Storage Rings, Lugano, 1988. Also, G. Guignard, Lecture Notes in Phys. 296, Springer-Verlag 1986, p. 3.

[6] E. Forest, SSC-30 (1985).

[7] R. D. Ruth, T. Raubenheimer, R. L. Warnock, IEEE Trans. Nucl. Sci. NS-32 (1985) 2206. Also, T. O. Raubenheimer and R. D. Ruth, SLAC-PUB-4370 (1987).

[8] J. Moser, Nachr. Akad. Wiss. Gottingen IIa, No.6, 87 (1955).

[9] A. Piwinski and A. Wrulich, DESY 76/07 (1976).

[10] R. L. Warnock and R. D. Ruth, Physica 26D (1987) 1.

[11] See for example, E. Forest, SSC-138 (1987).

[12] L. Schachinger and R. Talman, Part. Accel. 22 (1987) 35.

[13] R. D. Ruth, IEEE Trans. Nucl. Sci., NS-30 (1983) 2669.

[14] A. Dragt, AIP Proc. 87 (1982), p. 147.

[15] M. Berz, SSC-152 (1988), submitted to Part. Accel. 1988.

[16] E. Forest, M. Berz and J. Irwin, SSC-166 (1988), submitted to Part. Accel. 1988.

[17] K. L. Brown et al, SLAC-91 (1977).

[18] M. Berz, H. Wollnik and H. C. Hoffmann, Nucl. Instr. Meth. A 258 (1987) 402.

[19] A. J. Dragt et al, IEEE Trans. Nucl. Sci. NS-32 (1985) 2311.

[20] M. Berz, private communication (1988).

[21] M. Cornacchia and L. Evans, Part. Accel. 19 (1986) 125.

[22] J. Gareyte, Workshop on Aperture-Related Limitations in Storage Rings, Lugano, 1988.

[23] P. L. Morton et al, IEEE Tran. Nucl. Sci., NS-32, 2291 (1985).

[24] D. A. Edwards, R. P. Johnson, and F. Willeke, Part. Accel. 19, 145 (1986).

[25] E778 collaboration, submitted to the Phys. Rev. Lett, 1988. An interim report can be found in SSC-156 (1988).

[26] N. Merminga, these proceedings.

[27] J. Peterson, these proceedings.